Light Shifts in the Alkali Atoms*

B. S. MATHUR, H. TANG, AND W. HAPPER†
Columbia Radiation Laboratory, Columbia University, New York, New York
(Received 23 January 1968)

Quantitative formulas for computing the light shift due to virtual transitions in any alkali atom are presented. The theoretically calculated light shifts for Rb^{87} are compared with experimentally measured light shifts, and good quantitative agreement is obtained.

I. INTRODUCTION

ONE of the interesting results of early optical-pumping experiments was the discovery of "light shifts." It was found that in an optically pumped vapor certain ground-state transition frequencies underwent a shift which was proportional to the pumping light intensity. The first detailed experimental study of light shifts was carried out by Arditi and Carver.[1] They showed that ordinary resonance lamps could cause light shifts as large as several hundred hertz in the 0-0 transition frequencies of rubidium and cesium. Although these shifts are very small compared to the resonance frequencies, which are typically several gigahertz, they are, nevertheless, easily observable because of the extremely narrow linewidths which can be obtained in optical-pumping experiments.

The first systematic, theoretical study of the optical-pumping cycle was made by Barrat and Cohen-Tannoudji.[2] They showed that optical pumping can shift the ground-state transition frequencies of an atom by two distinct processes involving, respectively, real and virtual absorption of light. Light shifts due to real absorption of light occur when coherence from the atomic ground state can be transferred to the excited state upon absorption of a photon of pumping light. The excited-state coherence may then be passed on to the ground state, following spontaneous decay of the excited atom. Since the natural frequencies of the ground-state and excited-state coherences are not normally equal, a phase shift may occur in this coherence transfer cycle, and a shift in the effective ground-state transition frequency results. Light shifts due to real transitions are most pronounced when the resonant frequencies of the ground state differ from those in the excited state by an amount on the order of the spontaneous decay rate of the excited state. Light shifts due to virtual transitions are simply the Stark shifts caused by the oscillating electric field of the pumping light.

In this paper we shall be concerned with light shifts due to virtual transitions in the alkali atoms. Much of the impetus for this work was a desire to understand the effects of light shifts on the 0-0 hfs transition, which plays such an important role in various atomic-frequency standards.[3] Shifts of the hfs transition frequencies are due almost exclusively to virtual transitions because of the large disparity between the hfs splittings of the ground state and those of the excited state. Thus, we shall not be concerned with shifts due to real transitions although such shifts are important for the Zeeman transitions.

Recently,[4] it has been shown that one can considerably simplify the theory of light shifts due to virtual transitions by exploiting the rotational symmetry of the interaction of light with atoms. Thus, even though the hyperfine structure of the alkali atoms is rather complex, the light shift due to virtual transitions can be described by a simple light-shift operator

$$\delta\mathcal{E}=\delta\mathcal{E}_0+h\delta A\mathbf{I}\cdot\mathbf{J}-\boldsymbol{\mu}\cdot\delta\mathbf{H}+\delta\mathcal{E}_2 \qquad (1)$$

which is added to the unperturbed ground-state Hamiltonian of the atom. Each term in the light-shift operator produces a characteristic type of energy splitting of the ground-state sublevels of the atom (see Fig. 1).

The c.m. light shift, represented by $\delta\mathcal{E}_0$ in (1), is an equal downward (or upward) displacement of all of the ground-state sublevels. This type of shift was recently observed by Aleksandrov *et al.*[5] in potassium vapor illuminated by light from a Q-switched ruby laser. However, none of the transition frequencies between ground-state sublevels is affected by the c.m. light shift, so that this term is not of interest in most optical-pumping work.

The hfs light shift, which is represented by the term $h\delta A\mathbf{I}\cdot\mathbf{J}$ in (1), is entirely equivalent to a shift in the magnetic-dipole coupling constant of the alkali-atom ground state. Thus, the hfs light shift will not affect the frequencies of Zeeman transitions ($\Delta F=0$ transitions), but it will affect the frequencies of hfs transitions ($\Delta F=1$ transitions). Both the hfs light shift and the c.m. light shift are scalar quantities which depend on the spectral profile of the light but not on its polarization.

When the light beam has some degree of circular polarization, a Zeeman light shift can occur. The corresponding light-shift operator $-\delta\mathbf{H}\cdot\boldsymbol{\mu}$ can be thought of

* Work supported by the Joint Services Electronics Program (U. S. Army, U. S. Navy, and U. S. Air Force) under Contract No. DA-28-043 AMC-00099(E).
† Alfred P. Sloan Research Fellow.
[1] M. Arditi and T. R. Carver, Phys. Rev. **124**, 800 (1961).
[2] J. P. Barrat and C. Cohen-Tannoudji, J. Phys. (Paris) **22**, 329 (1961); **22**, 443 (1961).
[3] P. Davidovits and R. Novick, Proc. IEEE **54**, 155 (1966).
[4] W. Happer and B. S. Mathur, Phys. Rev. **163**, 12 (1967).
[5] E. B. Aleksandrov, A. M. Bonch-Bruevich, N. N. Kostin, and V. A. Khodovoi, Zh. Eksperim. i Teor. Fiz. Pis'ma v Redaktsiyu **3**, 85 (1966) [English transl.: JETP Letters **3**, 53 (1966)].

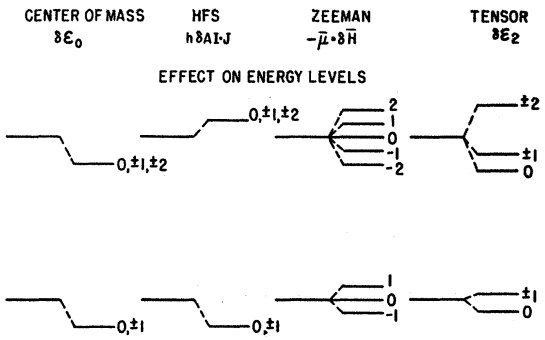

FIG. 1. The different types of light shift for an alkali atom.

as an interaction of the magnetic-dipole moment $\boldsymbol{\mu}$ of the atom with an effective magnetic field $\delta\mathbf{H}$ which is directed parallel or antiparallel to the light beam. Consequently, the Zeeman light shift will affect the Zeeman frequencies of the atom in exactly the same way as a small magnetic field $\delta\mathbf{H}$. Zeeman light shifts were first observed by Cohen-Tannoudji[6] in optically pumped mercury vapor. Several other interesting phenomena which are related to the Zeeman light shift have recently been observed. Van der Ziel *et al.*[7] have shown that the effective magnetic fields associated with circularly polarized light pulses from a Q-switched ruby laser are large enough to produce significant thermal polarization of paramagnetic ions. This phenomenon is one aspect of the inverse Faraday effect which was analyzed theoretically by Pershan *et al.*[8] Since the Zeeman light-shift operator has off-diagonal matrix elements, it is possible to induce real transitions between the Zeeman sublevels of the atomic ground state by illuminating the atoms with modulated, circularly polarized light. Such transitions, which may be thought of as optical double-quantum transitions, have been observed by Happer and Mathur.[9]

The tensor light shift, represented by the term $\delta\mathcal{E}_2$ in (1), is analogous to the tensor Stark shift which is caused by a static electric field.[10] In the light alkali atoms the tensor light shift is negligible with respect to the hfs and Zeeman light shifts because of the small excited-state hfs. However, in rubidium and cesium the hfs of the first excited states is well resolved, and the tensor light shift is not negligible.

The remainder of this paper is divided into two parts. In the theoretical section the general light-shift operators derived in Ref. 4 (hereafter denoted by HM) are evaluated for the alkali atoms, and theoretical light shifts for Rb^{87} are presented in graphical form. The notation used is the same as that of HM except where otherwise specified. In the experimental section of this paper, we report on quantitative experimental measurements of the light shift in Rb^{87} vapor illuminated by Rb^{85} pumping light.

II. THEORY

A. Light with a Broad Spectral Profile

In HM, effective operators were derived for a monochromatic light wave whose electric vector is

$$\mathbf{E}=\tfrac{1}{2}E_0[\mathbf{e}e^{i(\mathbf{k}\cdot\mathbf{r}-2\pi\nu t)}+\text{c.c.}]. \tag{2}$$

The average energy flux carried by such a wave is $c|E_0|^2/8\pi$. Light with a broad spectral profile may be represented by an ensemble of monochromatic waves with random phases. Let $\Phi(\nu)d\nu$ denote the energy flux carried by waves whose frequencies lie between ν and $\nu+d\nu$. Then the expressions derived in HM for the light-shift operator are applicable to light with a broad spectral profile provided that one makes the replacement

$$\frac{c|E_0|^2}{8\pi}\rightarrow\int_0^\infty d\nu\,\Phi(\nu). \tag{3}$$

B. hfs Light Shift

The hfs light-shift operator $\delta A\mathbf{I}\cdot\mathbf{J}$ will cause a shift $\delta\nu_{\text{hfs}}$ in the frequencies of the ground-state hfs transitions. Since the unperturbed splitting of the ground-state hfs levels is $\frac{1}{2}A(2I+1)$, one can immediately write

$$\delta\nu_{\text{hfs}}=\tfrac{1}{2}\delta A(2I+1)=\int_0^\infty S_{\text{hfs}}(\nu)\Phi(\nu)d\nu. \tag{4}$$

We can use (3) in conjunction with (III.14), (III.32), (A.26), (A.27), and (A.28) of HM to obtain an explicit expression for the hfs spectral-response function $S_{\text{hfs}}(\nu)$:

$$S_{\text{hfs}}(\nu)=-\frac{\lambda^2 r_0 f}{2\pi hc}\left(\frac{Mc^2}{2RT}\right)^{1/2}\text{Re}[\zeta^0(aa)-\zeta^0(bb)], \tag{5}$$

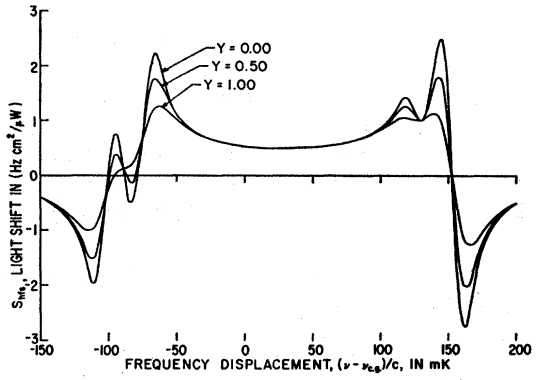

FIG. 2. The Rb^{87} hfs response function for 7947-Å D_1 light.

[6] C. Cohen-Tannoudji, Compt. Rend. **252**, 394 (1961).
[7] J. P. van der Ziel, P. S. Pershan, and L. D. Malmstrom, Phys. Rev. Letters **15**, 190 (1965).
[8] P. S. Pershan, J. P. van der Ziel, and L. D. Malmstrom, Phys. Rev. **143**, 574 (1966).
[9] W. Happer and B. S. Mathur, Phys. Rev. Letters **18**, 727 (1967).
[10] P. G. H. Sanders and J. R. P. Angel (to be published); A. Khadjavi, A. Lurio, and W. Happer, Phys. Rev. **167**, 128 (1968).

where

$$\zeta^0(F_gF_g)=2\sum_{F_e}(2F_e+1)W^2(J_eI1F_g;F_e\tfrac{1}{2})Z(F_eF_g). \quad (6)$$

Equations (4)–(6) are valid for any alkali atom with nuclear spin I and ground-state hfs levels $a=I+\frac{1}{2}$ and $b=I-\frac{1}{2}$. The profile function $Z(F_eF_g)$ is simply a Doppler-broadened resonance line, expressed in terms of a plasma-dispersion function[11] [see HM, (II.18)]:

$$Z(F_eF_g)\equiv Z[x(F_eF_g)+iy], \quad (7)$$

where

$$x(F_eF_g)=\frac{1}{\nu}\left(\frac{Mc^2}{2RT}\right)^{1/2}\{[\nu-\nu_{cg}]-[\nu(F_eF_g)-\nu_{cg}]\} \quad (8)$$

and

$$y=\left(\frac{Mc^2}{2RT}\right)^{1/2}\left(\frac{1/2\tau+\gamma_c}{2\pi\nu}\right). \quad (9)$$

The Rb^{87} hfs response function $S_{\rm hfs}(\nu)$ was evaluated for 7947-Å D_1 light and 7800-Å D_2 light, and the results are shown in Figs. 2 and 3, respectively. The absolute units of the curves, Hz cm$^2/\mu$W, were chosen to be consistent with convenient experimental units of measurement for light shifts (Hz) and resonance lamp light fluxes (μW/cm^2). The customary millikayser unit (1 mK$=10^{-3}$ cm^{-1}) of high-resolution optical spectroscopy was used to measure the displacement of the exciting light wave number ν/c from the wave number $\nu_{c.g.}/c$ of the center of gravity of the atomic absorption line. The 7947-Å response function (Fig. 2) shows a fairly complicated dependence on frequency because of the large hfs splittings of the $^2P_{1/2}$ excited state. The 7800-Å response function (Fig. 3) is less complex because of the smaller hfs splitting of the $^2P_{3/2}$ excited state. For a given light intensity and frequency displacement from the center of gravity of the resonance line, the light shift caused by 7800-Å D_2 light is approximately twice as large as that caused by 7947-Å D_1 light.

C. Effect of Buffer Gas on Response Curves

In HM it was assumed, for the sake of simplicity, that every collision of a pumped atom with a buffer-gas atom randomizes the phase of the optical coherence or quenches the excited state. Under these conditions, expressions (8) and (9) for the frequency-displacement parameter x and the broadening parameter y were easily obtained. Now we shall assume that (8) and (9) remain valid even when "soft" collisions occur, and we shall assume that any pressure shift may be accounted for by interpreting the center frequency $\nu_{c.g.}$ in (8) as the pressure-shifted center of gravity of the optical absorption line. Then

$$\nu_{c.g.}=\nu_0+\Delta\nu_0. \quad (10)$$

Here ν_0 is the unshifted center of gravity of the absorption line. The pressure shift $\Delta\nu_0$ may be expressed in terms of a pressure-shift cross section σ':

$$2\pi\Delta\nu_0=N\bar{v}\sigma'. \quad (11)$$

In (11), N is the buffer-gas number density and $\bar{v}$ is the rms relative velocity between an optically pumped atom (molecular weight m) and a colliding buffer-gas molecule (molecular weight M).

$$\bar{v}=[2RT(M+m)/Mm]^{1/2}. \quad (12)$$

In like manner we may define an optical pressure broadening cross section σ'':

$$\gamma_c=N\bar{v}\sigma''. \quad (13)$$

In the limit of very low buffer-gas pressure the pressure broadening and shifting of the optical-absorption lines will be negligible, and the broadening parameter y will be determined solely by the natural breadth $\Delta\nu_n$ and the Doppler breadth $\Delta\nu_D$ of the absorption line[12]:

$$y=\frac{1}{4\pi\nu_0\tau}\left(\frac{Mc^2}{2RT}\right)^{1/2}=(\ln 2)^{1/2}\Delta\nu_n/\Delta\nu_D. \quad (14)$$

For Rb^{87} vapor at room temperature, $y\approx10^{-3}$. Consequently, when no buffer gas is present (e.g., evacuated cells with coated walls), the frequency dependence of the light shift is well represented by response curves for $y=0$.

In the other extreme, when the pressure broadening is much greater than the natural linewidth, the broadening parameter becomes

$$y=\lambda\!\!\!^{-}N\sigma''[3(M+m)/2m]^{1/2} \quad (\lambda\!\!\!^{-}=c/2\pi\nu_0). \quad (15)$$

For rubidium in neon the pressure-broadening cross section is known [13] to be $\sigma''\approx10^{-14}$ cm^2. A buffer-gas pressure of 10 Torr of neon was used in the experimental work described in this paper to reduce the microwave

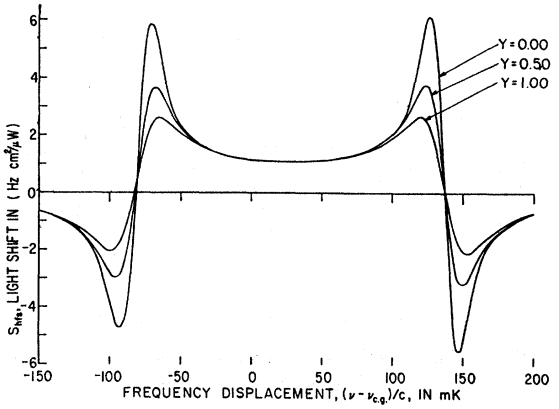

FIG. 3. The Rb^{87} hfs response function for 7800-Å D_2 light.

[11] B. D. Fried and S. D. Conte, *The Plasma Dispersion Function* (Academic Press Inc., New York, 1961).

[12] A. C. G. Mitchell and M. W. Zemansky, *Resonance Radiation and Excited Atoms* (Cambridge University Press, New York, 1961), pp. 99, 100.

[13] S. Ch'en and M. Takeo, Rev. Mod. Phys. **29**, 20 (1957).

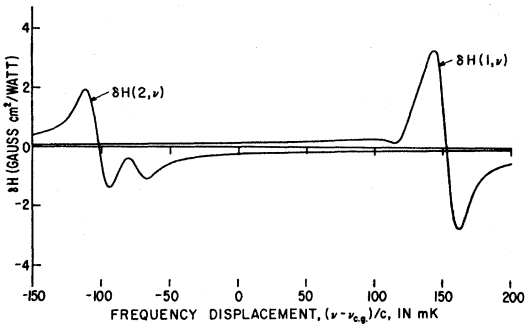

FIG. 4. The effective magnetic-field response function for 7947-Å D_1 light ($y=0$).

Doppler effect.[14] For this pressure the broadening parameter (15) is $y\approx 0.1$.

The response curves in Figs. 2–7 were calculated for various values of the broadening parameter y corresponding to various buffer-gas pressures. The response curves are strongly dependent on y near the center of the optical-absorption lines, but the wings of the response curves are relatively insensitive to the buffer-gas pressure.

D. Effect of Temperature on Response Curves

Both the frequency-displacement parameter x and the broadening parameter y, defined in (8) and (9), respectively, depend on the temperature T of the optically pumped vapor. Explicit calculations of the change in the response curves as the temperature varied from 300 to 400°K showed that temperature variation in this range had a negligible effect on the response curves. All of the response curves reproduced in the figures were calculated for $T=300$°K—about room temperature.

E. Zeeman Light Shift

The Zeeman light-shift operator $-\delta\mathbf{H}\cdot\boldsymbol{\mu}$ can be thought of as describing the interaction of the magnetic-dipole moment $\boldsymbol{\mu}$ of the atom with an effective magnetic field $\delta\mathbf{H}$. The effective field is present when the light has some degree of circular polarization. In the alkali atoms one must describe the Zeeman light shift in the two different ground-state Zeeman multiplets by two different magnetic fields, since the spectral profile of the light may be such that one Zeeman multiplet is much more strongly influenced by virtual transitions than the other. From (III.18) of HM we find that the effective magnetic field $\delta\mathbf{H}(F_g)$ for the ground-state Zeeman multiplet F_g is

$$\delta\mathbf{H}(F_g)=\mathbf{s}\int_0^\infty \delta H(F_g\nu)\phi(\nu)d\nu, \tag{16}$$

where

$$\delta H(F_g\nu)=\frac{\lambda^2 r_0 f}{16\pi g_J\mu_0}\left(\frac{M}{2RT}\right)^{1/2} \times[11-4J_e(J_e+1)]\mathrm{Re}\zeta^1(F_gF_g) \tag{17}$$

and

$$\zeta^1(F_gF_g)=\frac{\sum_{F_e}(-1)^{F_e-F_g}(2F_e+1)W(11F_gF_g;1F_e)W^2(J_eF_e\tfrac{1}{2}F_g;I1)Z(F_eF_g)}{W(F_g1I\tfrac{1}{2};F_g\tfrac{1}{2})W(11J_e\tfrac{1}{2};1\tfrac{1}{2})}. \tag{18}$$

The vector $\mathbf{s}$ is the average spin of the photons, and, consequently, $\mathbf{s}$ must be parallel or antiparallel to the direction of the light beam. When the light beam is in a pure state of polarization, represented by a polarization vector $\mathbf{e}$ [e.g., Eq. (2)],

$$\mathbf{s}=i\mathbf{e}\times\mathbf{e}^*. \tag{19}$$

For right circularly polarized light, $\mathbf{s}$ is a unit vector parallel to the beam direction; for left circularly polarized light, $\mathbf{s}$ is a unit vector antiparallel to the beam direction. For all other cases $\mathbf{s}$ lies between these two extreme values.

Equations (16)–(18) are valid for any alkali atom. The frequency response function $\delta H(F_g\nu)$ of the effective magnetic fields has been plotted for Rb^{87} in Figs. 4 and 5. Just as in the hfs light shift, the effects of the excited-state hfs are much more prominent for 7947-Å light than for 7800-Å light. For a given light intensity and frequency displacement, the effective magnetic field produced by 7800-Å light is approximately equal in magnitude and opposite in sign from the corresponding effective field produced by 7947-Å light.

The use of the effective-magnetic-field response curves is best illustrated by an example. Suppose that a 100-μW/cm² beam of right circularly polarized 7947-Å light is incident along the z axis which is defined by a small static magnetic field. If the spectral profile of the incident light is strongly peaked at $(\nu-\nu_{c.g.})/c=-50$

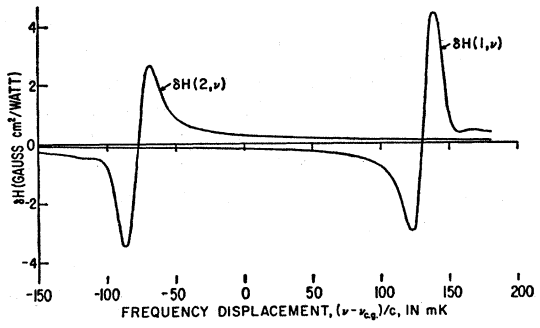

FIG. 5. The effective magnetic-field response function for 7800-Å D_2 light ($y=0$).

[14] R. H. Dicke, Phys. Rev. 89, 472 (1953).

mK, we may use Fig. 4 to determine that $\delta H(2)=-55.5$ μG and $\delta H(1)=+11.2$ μG. The Larmor frequencies of both the $F=2$ and $F=1$ Zeeman multiplets are known[15] to be approximately 700 kHz/G, so that the Larmor frequency of the $F=2$ multiplet is *decreased* by 39 Hz while the Larmor frequency of the $F=1$ multiplet is *increased* by 8 Hz.

We should emphasize that this simple calculation of the Zeeman light shift due to virtual transitions is completely equivalent to the rather cumbersome method given in Ref. 2, where no attempt was made to evaluate the sum over intermediate states. Other advantages of the effective-field concept are that it allows one to see at a glance how the light shift depends on the angle between the light beam and the static magnetic field. For low light intensity the Zeeman light shift goes to zero when the circularly polarized light is incident at right angles to the direction of the static magnetic field, since then the small effective magnetic field adds in quadrature to the static field. As mentioned in the Introduction, the Zeeman resonance frequencies may also be shifted by real transitions, and these are not accounted for by the effective magnetic field.

F. Tensor Light Shift

When the excited-state hfs of the alkali atoms is much smaller than the Doppler width of the absorption lines, the tensor light shift will be negligible in comparison with the other types of light shift. However, in Rb^{87} the hfs of the first excited states is comparable with the Doppler widths, and, under some circumstances, the tensor light shift may be noticeable. The tensor light-shift operator $\delta\mathcal{E}_2$ will cause a shift $\delta\nu_t$ in the frequency of the field-independent 0-0 transition which is given by

$$h\delta\nu_t=\langle 2,0|\delta\mathcal{E}_2|2,0\rangle-\langle 1,0|\delta\mathcal{E}_2|1,0\rangle. \quad (20)$$

Using Eqs. (II.38), (III.1), and other expressions from HM, one can write

$$\delta\nu_t=E_0^2\int_0^\infty S_2(\nu)\Phi(\nu)d\nu, \quad (21)$$

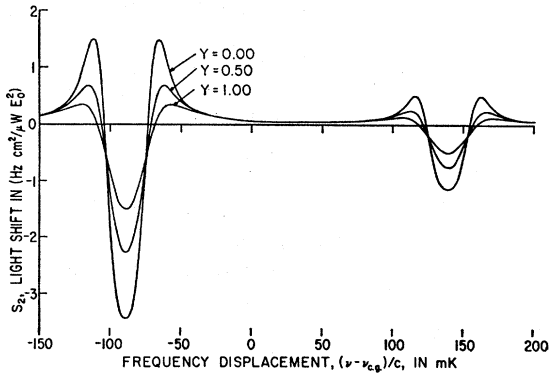

FIG. 6. The tensor response function for 7947-Å D_1 light.

[15] F. A. Franz, Phys. Rev. **141**, 105 (1966).

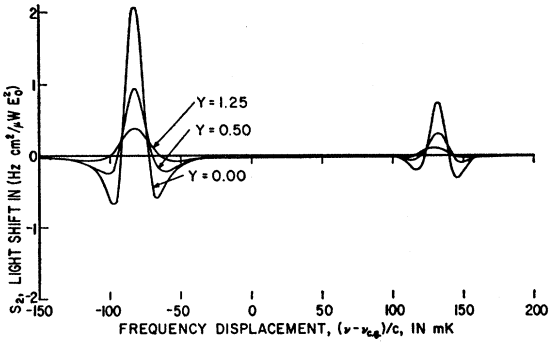

FIG. 7. The tensor response function for 7800-Å D_2 light.

where

$$S_2(\nu)=\frac{2\pi}{hc}\sum_{F_g}\left[\frac{5F_g(F_g+1)}{(2F_g-1)(2F_g+1)(2F_g+3)}\right]^{1/2}\times\mathrm{Re}A^2(F_gF_g)(-1)^{I+1/2-F_g} \quad (22)$$

and

$$A^2(F_gF_g)=\frac{3\lambda^2r_0f}{4\pi^2}\left(\frac{Mc^2}{2RT}\right)^{1/2}(2F_g+1)\sum_{F_e}(2F_e+1)\times W(11F_gF_g;2F_e)W^2(J_eF_e\tfrac{1}{2}F_g;I1)\times Z(F_eF_g)(-1)^{F_e-F_g-1}. \quad (23)$$

The quantity E_0^2 in (21) is a polarization tensor constructed from the polarization vector **e** of the exciting light:

$$E_0^2=1/\sqrt{6}-(\sqrt{\tfrac{3}{2}})|e_Z|^2. \quad (24)$$

Thus, the tensor light shift of the field-independent transition is present even for an unpolarized light beam. It vanishes only for completely isotropic light.

The explicit form of the Rb^{87} response function is

$$S_2(\nu)=-\frac{3\lambda^2r_0f}{2\pi h}\left(\frac{M}{2RT}\right)^{1/2}\sum_{F_e}(-1)^{F_e}(2F_e+1)\times[5(2/7)^{1/2}W(1122;2F_e)W^2(J_eF_e\tfrac{1}{2}2;\tfrac{3}{2}1)\times\mathrm{Re}\,Z(F_e2)+(3\sqrt{\tfrac{2}{3}})W(1111;2F_e)\times W^2(J_eF_e\tfrac{1}{2}1;\tfrac{3}{2}1)\,\mathrm{Re}Z(F_e1)]. \quad (25)$$

Expression (25) was evaluated, and the results are shown in Figs. 6 and 7.

Since the tensor shift vanishes when the excited-state hyperfine splittings go to zero, the 7800-Å tensor shift is considerably smaller than the 7947-Å tensor shift. (Note the expanded scale of Fig. 7.)

III. EXPERIMENTAL

A. Choice of Isotope and Transition

In order to make a quantitative, experimental test of the light-shift theory which was presented in Sec. II,

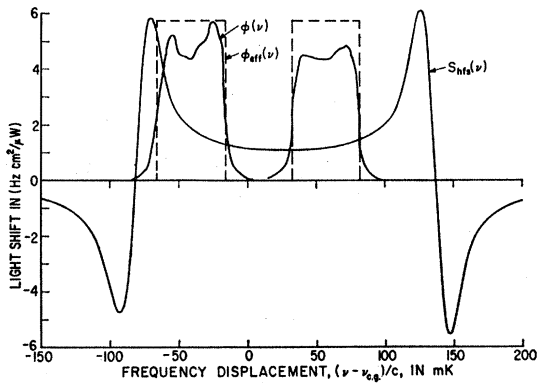

FIG. 8. Method of estimating the light shift of the Rb^{87} 0-0 transition caused by Rb^{85} light.

it is necessary to know the spectral profile $\Phi(\nu)$ of the light, the polarization of the light, the light shift $\delta\nu$ of some transition frequency, and the parameters which determine the response curve, such as the buffer-gas pressure, the optical pressure broadening, pressure-shift cross sections, etc. Since no high-resolution spectroscopic instrument was available when these experiments were undertaken, it was necessary to choose an arrangement which would be fairly insensitive to the spectral profile of the lamp. Consequently, light from a Rb^{85} lamp was used to illuminate a vapor of Rb^{87} atoms. The reason for this choice is evident from Fig. 8, where a typical spectral profile for a Rb^{85} resonance lamp is shown superimposed on the hfs light-shift response curve of Rb^{87}. The $F=3$ hfs component of the Rb^{85} emission line slightly overlaps the $F=2$ component of the Rb^{87} absorption line, so that Rb^{85} light will tend to pump Rb^{87} atoms into the lower hfs level $F=1$. However, most of the spectral profile of the Rb^{85} lamp is well removed from the Rb^{87} absorption lines. This is a desirable situation, since in these regions the response curves are slowly varying and quite insensitive to buffer-gas pressure or to the temperature of the vapor. In addition, the portions of the Rb^{85} spectral profile which account for most of the light shift will not be significantly attentuated by Rb^{87} vapor.

Two different types of transition, Zeeman transitions ($\Delta F=0$) and hfs transitions ($\Delta F=1$), can be used to investigate light shift. All of the Zeeman transitions are magnetic-field–dependent, so that elaborate magnetic shielding and well-regulated static magnetic fields are required in order to obtain stable, narrow lines. Zeeman transitions may also be subject to light shifts due to real transitions, and the light shifts due to virtual transitions are usually quite different for the two different ground-state multiplets. Furthermore, all of the Zeeman transitions occur at approximately the same frequency, so that the resonance line shapes are quite complicated.

In contrast, the 0-0 hfs transition is field-independent to first order, so that no special magnetic shielding is required. Furthermore, the 0-0 transition is not affected by Zeeman light shifts or by shifts due to real transitions. Only the hfs light shift and the tensor light shift need to be taken into account, and the tensor light shift is small. The 0-0 resonance can be separated from the other hfs resonances by a small magnetic field. Thus, for absolute comparison with theory, it is most sensible to measure the light shifts of the 0-0 transition frequency.

B. Predicted Light Shift

Experimentally, we were able to measure the total light flux

$$\Phi_0=\int_0^\infty \Phi(\nu)d\nu \tag{26}$$

directly with a thermopile. However, we had no direct information about the shape of the spectral profile, and it was necessary to make certain assumptions about the spectral profile in order to be able to predict the light shift. These assumptions, which are in accord with most published data on lamps similar to the one that we used,[3,16,17] were as follows:

(a) The total intensity of the $F=3$ hfs component was approximately equal to the total intensity of the $F=2$ hfs component.

(b) The width of each hfs component was about 50 mK.

(c) The true spectral profile of the lamp, $\Phi(\nu)$, can be replaced in expressions such as (4) by an effective spectral profile $\Phi_{eff}(\nu)$ which consists of two identical 50-mK-wide rectangles centered on the $F=3$ and $F=2$ emission lines of a Rb^{85} lamp.

These assumptions are illustrated in Fig. 8. Although one cannot expect precise agreement between experiment and theory with such a coarse approximation of the lamp profile, one should obtain considerably better than order-of-magnitude agreement.

The convolution (4) of the effective lamp profile with the hfs light-shift response curve was evaluated numerically to yield

$$\delta\nu_{hfs}=0.80\Phi_0(D_1)+1.68\Phi_0(D_2). \tag{27}$$

The hfs light shift $\delta\nu_{hfs}$ will be in hertz if the intensities Φ_0 are expressed in $\mu W/cm^2$. The theoretical tensor light shift $\delta\nu_t$ can be calculated from (21) in like manner:

$$\delta\nu_t=E_0^2[0.30\Phi_0(D_1)-0.08\Phi_0(D_2)]. \tag{28}$$

Unpolarized Rb^{85} light, propagating along the direction of the static magnetic field, was used to cause light shifts in these experiments. Under such conditions, the appropriate value of the polarization tensor component E_0^2 is [see Eq. (24)]

$$E_0^2=1/\sqrt{6}. \tag{29}$$

[16] H. M. Gibbs and R. J. Hull, Phys. Rev. **153**, 132 (1967).
[17] W. E. Bell, A. L. Bloom, and J. Lynch, Rev. Sci. Instr. **32**, 688 (1961).

The total theoretical light shift of the 0-0 transition frequency is then

$$\delta\nu=\delta\nu_{\rm hfs}+\delta\nu_t=0.92\Phi_0(D_1)+1.65\Phi_0(D_2). \quad (30)$$

The effect of the tensor light shift is to increase the light shift caused by D_1 light by about 10% and to decrease the light shift caused by D_2 light by about 1% from the values which would result from the hfs light shift alone. The light shift caused by a given total intensity of 7800-Å D_2 light should be 1.8 times greater than the light shift caused by the same total intensity of 7947-Å D_1 light.

C. Apparatus

The apparatus used to measure the 0-0 light shift is shown in Fig. 9. The light source was a Varian X49-609 spectral lamp.[17] The Pyrex lamp bulbs, which were about 1 cm in diam, were filled with 99.5%-separated Rb^{85} isotope and about 3 Torr of krypton. The intensity of the lamps varied by no more than 10% from day to day, and intensity fluctuations over the 1-h period necessary to complete a set of measurements did not normally exceed 3%. Interference filters were used to isolate either the 7947-Å or the 7800-Å resonance light. The filters had a bandwidth of 85 Å at half-maximum transmission and a peak transmission of about 50%. The incident light was further attentuated by Corning glass neutral-density filters to obtain a variable light intensity at the absorption cell. The absorption cell was kept at room temperature so that the attentuation of the light in the cell due to resonance absorption was small except for frequencies near the centers of the Rb^{87} optical-absorption lines. Such frequencies have very little effect on the hfs light shift.

The absorption cells were constructed of low-loss Corning 707 glass. They were coated with paraffin, and filled with 99%-separated Rb^{87} isotope and 10 Torr of neon or nitrogen buffer gas. The cells were placed inside a cylindrical microwave cavity which was excited in the TE_{011} mode at 6835 GHz. A small axial magnetic field was applied to the cavity with Helmholtz coils. This field removed the degeneracy of the hfs transition frequencies, and it could be used for fine tuning of the 0-0 transition frequency. It also ensured that the 0-0 transition was driven most strongly in atoms near the axis of the cavity where the microwave field was large and parallel to the static field. The cavity tuning could be adjusted slightly by varying the position of the cavity base.

The microwaves were generated by harmonic multiplication of the 999 225-Hz signal from a National Bureau of Standards (NBS) crystal-controlled oscillator. The signal was first multiplied to 60 MHz by a chain of vacuum-tube multipliers. The 60-MHz signal was applied to a varactor diode which was mounted in a waveguide, and the desired 6835-MHz signal was isolated by passing the harmonics from the varactor diode through a tuned cavity resonator. The microwaves then

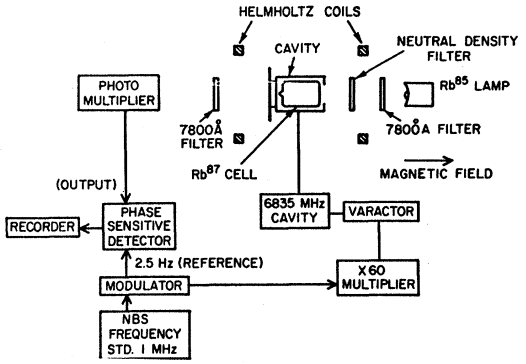

FIG. 9. Apparatus.

passed through an attenuator and into the absorption cavity. A maximum 6835-MHz signal power of about 10^{-7} W could be obtained in this way, and this power was more than adequate for the experiment. Under normal operating conditions the microwave power was attenuated by 30 dB before reaching the absorption cavity. The linewidth of the 0-0 resonance was then about 200 Hz.

The frequency of the NBS crystal-controlled oscillator could be tuned slightly by changing the capacitative loading of the crystal. This was accomplished with a variable capacitor whose value could be read on a vernier dial. The microwave frequency corresponding to a given setting of the vernier dial was calibrated directly by measuring the quadratic dependence of the 0-0 transition frequency on the magnetic field. The dependence of the microwave frequency on the vernier setting was linear to 1%, and the calibration was found to be

$$1 \text{ vernier division}=8.34 \text{ Hz}.$$

The resonance curves were recorded by slowly sweeping the vernier capacitance through its 100-division range with a synchronous motor. The transmission of the Rb^{85} light through the cavity was simultaneously monitored with a photomultiplier tube. The microwaves were chopped at a low frequency (2–3 Hz), and the resulting low-frequency signal from the photomultiplier tube was detected with a PAR phase-sensitive detector. The output of the phase-sensitive detector was recorded on a chart recorder, and fiducial marks were entered on the chart paper at 25, 50, and 75 vernier divisions so that the centers of the resonance curves could be accurately determined by extrapolation. To eliminate systematic error due to time lags in the recording system, several forward and backward sweeps of the vernier dial were made for each light intensity.

D. Inhomogeneous Light Flux

Since the atoms are essentially frozen in place due to the presence of buffer gas, and since the magnitude of the light shift depends on the light intensity, an inhomogeneous broadening of the microwave resonance

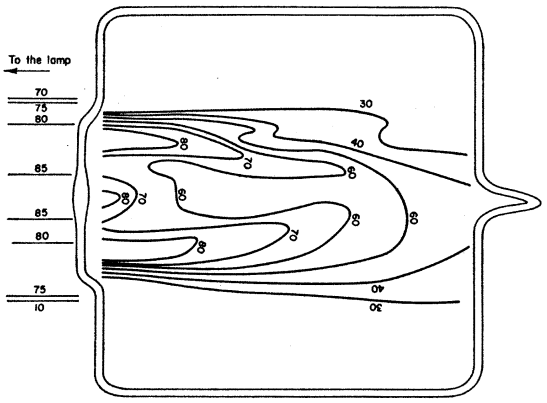

FIG. 10. Contours of constant light intensity within a large absorption cell. The intensity is measured in arbitrary units.

line will occur if the light intensity is not constant throughout the absorption cell. In our initial experiments we used large absorption cells which completely filled the microwave cavity. A contour map of the light intensity inside such a cell is shown in Fig. 10. The variations of the light intensity within the absorption cell were partially due to the angular divergence of the light beam as it traversed the absorption cell. A second, unanticipated source of flux inhomogeneity was a focusing of the light beam by the curved end wall of the absorption cell. In order to reduce the inhomogeneous broadening of the resonance lines, shorter cells with flat end walls were used. Measured linewidths for these two types of cells are shown in Fig. 11. The average light flux and the microwave power were approximately the same in both cases. The linewidth in the short cell is about three times narrower than the linewidth in the large cell.

The total light intensity was measured with an Eppley bismuth-silver thermopile (serial No. 7848, calibration: 7.5 μW/cm^2 μV) in a fiducial plane directly in front of the cells (see Fig. 11). By examining light-intensity maps such as the one shown in Fig. 10, it was estimated that the effective light intensity at the center of the cavity was about 60% of the measured light intensity in the fiducial plane. This estimate is uncertain by about 10%, but a more precise estimate of the effective intensity would be quite involved because of the complicated dependence of the detected signal on the path of the light rays through the cell and on the microwave mode structure within the cavity.

E. Results

Light-shift measurements were repeated many times in several different absorption cells. The measurements were reproducible to within 5%, and some typical results for D_1 and D_2 light are shown in Fig. 12. The solid lines are the theoretically predicted light shifts of Sec. III B. It was found that the light shift depends upon the operating conditions of the lamp such as bulb temperature, rf power input, etc. This is not surprising since one expects the spectral profile of the light to depend on the lamp conditions. The experimental points indicated by circles in Fig. 12 were obtained with the lamp operating at the designed power level and bulb temperature. The experimental points indicated by triangles in Fig. 12 were obtained with a higher bulb temperature in the lamp. Although more total light intensity was obtained from a hot lamp, the light shift per unit light intensity was consistently about 15% less than the light shift caused by light from the same lamp operating under the designed conditions. We hope to obtain direct measurements of the spectral profile of the lamp in the near future. These should allow us to understand in detail the variation of the measured light shift with lamp conditions. For given lamp conditions the D_2 light shift was always found to be 1.8(1) times larger than the D_1 light shift, in agreement with the predictions of Sec. III B. The absolute agreement between experiment and theory is also satisfactory when one considers the uncertainties associated with the spectral profile (Sec. III B) and the inhomogeneous light intensity (Sec. III D).

IV. CONCLUSIONS

We have discussed the light shifts due to virtual transitions in the alkali atoms in terms of the light-shift operator. These shifts can be classified into three types: hfs, Zeeman, and tensor light shifts. The tensor light shift is normally much smaller than the other two types. An important advantage of the light-shift operator is that it clearly separates the roles of the atomic observables, the spectral profile, and the polarization of the light. The shifts are proportional to the convolution of the spectral profile of the light with an appropriate spectral-response function. Examples of such spectral-response functions are shown graphically for Rb^{87}. The pronounced dependence of the response functions on the cross sections for pressure broadening and shifting of the

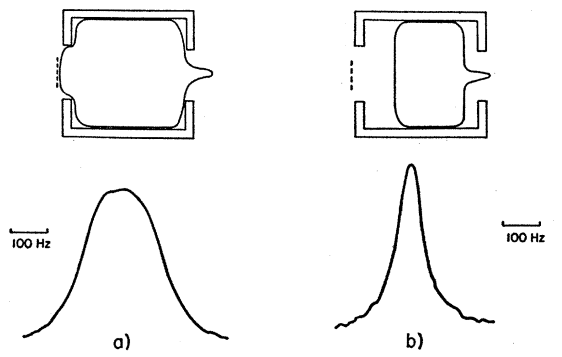

FIG. 11. (a) Inhomogeneously broadened linewidth in a large absorption cell. (b) Linewidth in a shorter cell with flat end walls. The absolute light intensity was measured in the fiducial plane marked with dashed lines, and intensity contour maps such as the one in Fig. 9 were used to estimate the effective light intensity within the cell.

optical-absorption lines emphasizes the need for better experimental values of such cross sections.

Experimental measurements of the light shifts of the 0-0 transition frequency in Rb^{87} are in good quantitative agreement with theory. Thus the theory should serve as a useful guide in the design of optically pumped alkali-vapor frequency standards.

Although extensive empirical data on light shifts were obtained by Arditi and Carver,[1] it is not possible to make any quantitative comparison between their data and the theory of this paper because there is no information on the absolute intensity and spectral profile of the light used in their experiments. However, many of the qualitative features observed by Arditi and Carver are in accord with the theory of this paper. In particular, their observation that the light shift was less pronounced at higher buffer-gas pressures is understandable since the light-shift response functions (e.g., Fig. 2) decrease in magnitude at higher buffer-gas pressures.

Basically, the light shifts depend only on the oscillator strength of the resonance line involved in the virtual transitions. When strong, tunable sources of optical radiation become available, it will be possible to measure oscillator strengths to unprecedented accuracy by measuring light shifts produced by light of known intensity and frequency. This is not surprising since, in the hook method of Roschdestwensky,[18] one uses the "converse" of light shifts, anomalous dispersion, to measure oscillator strengths. However, whereas a knowledge of the atomic density is required in the hook method, the light-shift method would be independent of atomic density, in common with the Hanle method,[19] the phase-shift method,[20] and direct observation of the exponential decay of excited atoms.[21] All of the density-independent methods except for the light-shift method actually yield an atomic lifetime and not necessarily an oscillator strength. Thus the light-shift method would combine all of the best features of existing techniques as well as offering one the attractive experimental option of using a frequency measurement to determine an oscillator strength.

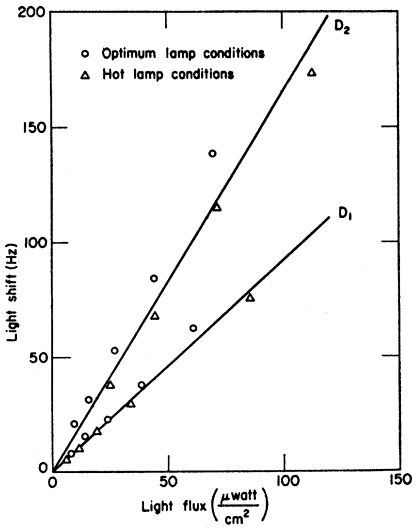

FIG. 12. Typical results for D_1 and D_2 light. The solid lines are the estimates of Sec. III B; ○, experimental data for normal lamp conditions; △, experimental data for a hot lamp.

ACKNOWLEDGMENTS

The authors would like to thank R. Brignoli and C. Sofes for assistance in the experiments, and J. Clendenin for writing a computer program to evaluate the response functions. A plasma-dispersion subroutine was lent to us by Peter Korn. Finally, we are sincerely grateful to Professor R. Novick, who provided the initial stimulus for this work.

[18] D. Roschdestwensky, Ann. Phys. (Paris) **39**, 307 (1912).
[19] A. Lurio, R. L. deZafra, and R. J. Goshen, Phys. Rev. **134**, 1198 (1964).
[20] P. T. Cunningham and J. K. Link, J. Opt. Soc. Am. **57**, 1000 (1967).
[21] B. P. Kibble, G. Copley, and L. Krause, Phys. Rev. **153**, 9 (1967).